

# PROCEEDINGS OF SPIE

[SPIEDigitalLibrary.org/conference-proceedings-of-spie](https://SPIEDigitalLibrary.org/conference-proceedings-of-spie)

## Urinary bladder cancer T-staging from T2-weighted MR images using an optimal biomarker approach

Chuang Wang, Jayaram K. Udupa, Yubing Tong, Jerry Chen, Sriram Venigalla, et al.

Chuang Wang, Jayaram K. Udupa, Yubing Tong, Jerry Chen, Sriram Venigalla, Dewey Odhner, Thomas J. Guzzo, John Christodouleas, Drew A. Torigian, "Urinary bladder cancer T-staging from T2-weighted MR images using an optimal biomarker approach," Proc. SPIE 10575, Medical Imaging 2018: Computer-Aided Diagnosis, 105752D (27 February 2018); doi: 10.1117/12.2294550

**SPIE.**

Event: SPIE Medical Imaging, 2018, Houston, Texas, United States

# Urinary bladder cancer T-staging from T2-weighted MR images using an optimal biomarker approach

Chuang Wang<sup>a</sup>, Jayaram K. Udupa<sup>a</sup>, Yubing Tong<sup>a</sup>, Jerry Chen<sup>b</sup>, Sriram Venigalla<sup>b</sup>, Ronac Mamtani<sup>d</sup>, Dewey Odhner<sup>a</sup>, Thomas J. Guzzo<sup>c</sup>, John Christodouleas<sup>b\*</sup>, Drew A. Torigian<sup>a\*</sup>

<sup>a</sup>Medical Image Processing Group, 602 Goddard Building, 3710 Hamilton Walk, Department of Radiology, University of Pennsylvania, Philadelphia, PA 19104

<sup>b</sup>The Perelman Center for Advanced Medicine, 3400 Civic Center Blvd., Department of Radiation Oncology, University of Pennsylvania, Philadelphia, PA 19104

<sup>c</sup>The Perelman Center for Advanced Medicine, 3400 Civic Center Blvd., Department of Urology, University of Pennsylvania, Philadelphia, PA 19104

<sup>d</sup>The Perelman Center for Advanced Medicine, 3400 Civic Center Blvd., Department of Medical Oncology, University of Pennsylvania, Philadelphia, PA 19104

(\*These are both senior authors with equal contribution.)

## ABSTRACT

Magnetic resonance imaging (MRI) is often used in clinical practice to stage patients with bladder cancer to help plan treatment. However, qualitative assessment of MR images is prone to inaccuracies, adversely affecting patient outcomes. In this paper, T2-weighted MR image-based quantitative features were extracted from the bladder wall in 65 patients with bladder cancer to classify them into two primary tumor (T) stage groups: group 1 – T stage  $\leq$  T2, with primary tumor locally confined to the bladder, and group 2 – T stage  $>$  T2, with primary tumor locally extending beyond the bladder. The bladder was divided into 8 sectors in the axial plane, where each sector has a corresponding reference standard T stage that is based on expert radiology qualitative MR image review and histopathologic results. The performance of the classification for correct assignment of T stage grouping was then evaluated at both the patient level and the sector level. Each bladder sector was divided into 3 shells (inner, middle, and outer), and 15,834 features including intensity features and texture features from local binary pattern and gray-level co-occurrence matrix were extracted from the 3 shells of each sector. An optimal feature set was selected from all features using an optimal biomarker approach. Nine optimal biomarker features were derived based on texture properties from the middle shell, with an area under the ROC curve of AUC value at the sector and patient level of 0.813 and 0.806, respectively.

**Keywords:** Optimal biomarker approach, feature extraction, bladder cancer staging, magnetic resonance imaging (MRI)

## 1. INTRODUCTION

Bladder cancer is among the top 10 most common carcinomas. In the United States, an estimated 79,030 newly diagnosed cases (60,490 men and 18,540 women) occurred in 2017, and an estimated 16,870 patients will die of bladder cancer [1]. A major determinant of the type of treatment patients with bladder cancer will receive is whether the primary tumor is confined to the bladder (primary tumor (T) stage  $\leq$  T2), which likely requires locoregional therapies only (such as cystectomy or radiation therapy), or has spread beyond the bladder (T stage  $>$  T2 which generally requires systemic chemotherapy).

In clinical practice, computed tomography (CT), magnetic resonance imaging (MRI), and positron emission tomography (PET) imaging are often used to determine the locations and extent of tumor in patients with bladder cancer to stage the disease and to plan treatment [11]. In particular, MRI has high soft tissue resolution and multiplanar capabilities. Furthermore, MRI does not expose patients to ionizing radiation. Therefore, MRI is used as an important staging modality in clinical practice to stage patients with bladder cancer to help plan treatment. Different sequences of MR

images provide different types of image contrast, which can facilitate the local staging, including T2-weighted images that can depict the tumor well.

However, qualitative assessment of MR images is prone to inaccuracies which commonly results in the over-treatment of patients misclassified as stage  $> T2$  and the under-treatment of patients misclassified as stage  $\leq T2$ . Therefore, it is important to develop a quantitative method of assessing MR images to accurately predict bladder cancer T stage. In this study, we utilized an optimal biomarker approach to select those quantitative imaging features extracted from T2-weighted MR images in patients with primary bladder cancer which best separate patients into two T stage groups: group 1 – T stage  $\leq T2$ , and group 2 – T stage  $> T2$ .

An optimal biomarker approach is employed to predict urinary bladder cancer T stage group at the sector and patient level based on pelvic axial T2-weighted MR images. The problem addressed in the current study is more challenging than staging based only on images acquired in previously untreated patients. Image-based features are extracted from 8 sectors and 3 shells placed about the urinary bladder in all patients to predict bladder cancer T stage at both sector and patient levels.

The rest of this paper is organized as follows. In Section 2, a brief description of our methodology which includes data preprocessing, bladder shell delineation, feature extraction, optimal biomarker selection, and cross-validation. The experimental results are reported in Section 3. The conclusions are summarized in Section 4.

## 2. METHOD

### 2.1 Image data preprocessing

In this study, all image data sets were trimmed in a consistent manner for the body region by using the CAVASS system [3]. The axial slice with maximal cross-sectional coverage through the femoral heads was selected. Then, a region of interest (ROI) rectangular box was specified along the lateral edges of the femoral heads and along the anterior and posterior boundaries of the pelvic wall skeletal musculature as shown in Figure 1a. All axial slices through the pelvis were then trimmed by the same ROI. The two axial slices within 10 mm of the superior and inferior aspects of the urinary bladder were selected as the superior and inferior boundaries of the ROI, respectively.

In order to ensure the same tissue-specific numeric meaning for image voxel intensity values, all images were first corrected for intensity non-uniformities and then standardized [2] according to a standard intensity scale. Additional pelvic axial T2-weighted fast spin echo MR image datasets from 10 adult patients without bladder cancer or other known bladder pathology were also utilized as reference images for calibrating the MR image intensity standardization process [2]. The parameters of the scale were estimated by using these 10 “normal” image data sets.

### 2.2 Bladder shell delineation

The visual appearance and the image content of urine within the bladder lumen compared to the bladder wall and perivesical fat on T2-weighted MR images are different as shown in Figure 1b, and the differential features extracted from these different regions are likely related to bladder cancer T stage.

In order to classify patients into the two T stage groups, three shells around the bladder are defined as shown in Figure 1c. These include an inner shell which contains very high T2-weighted signal intensity urine within the bladder lumen, a middle shell which contains low signal intensity bladder wall detrusor muscle including higher signal intensity foci of bladder tumor, and an outer shell which contains high signal intensity perivesical fat within 10 mm of the outer bladder wall. The inner and outer boundaries of the bladder wall were manually drawn using CAVASS software on the axial T2-weighted MR images by two individuals (JC, SV), so that the 3 shells could then be created.

Subsequently, the bladder was divided on all axial slices into 8 equal sectors (S1-S8) centered upon the geometric center of the urinary bladder as shown in Figure 1d. This enables comparison of the proposed approach for bladder cancer T staging at both the patient level and the radial sector level. Representative T2-weighted MR Images from a patient with urinary bladder cancer showing 8 sectors (bounded by red lines) and 3 shells (bounded by red, dark blue, and light blue curves) are shown in Figure 2.

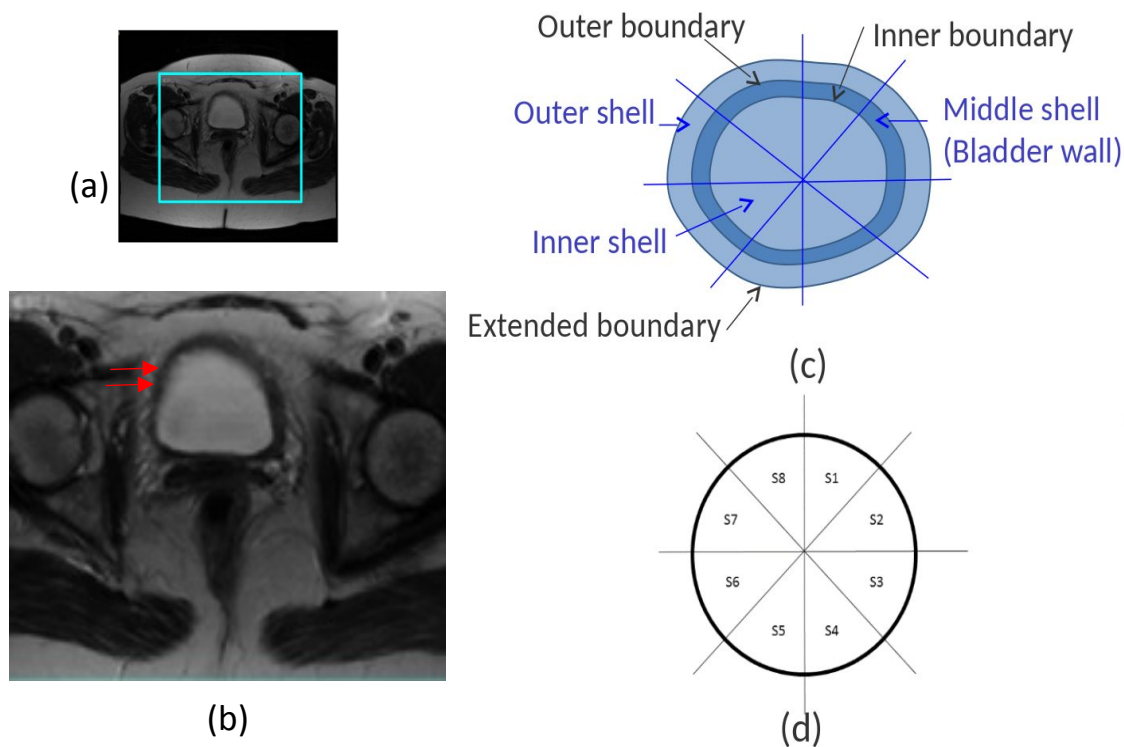


Figure 1. (a) An example region of interest (ROI) rectangular box on a T2-weighted MR image. (b) The visual appearance of bladder wall (arrows) on a T2-weighted MR image. (c) Schematic diagram of three-layer shell-like structure including boundaries and 8 radial sectors. (d) 8 radial sectors (S1-S8).

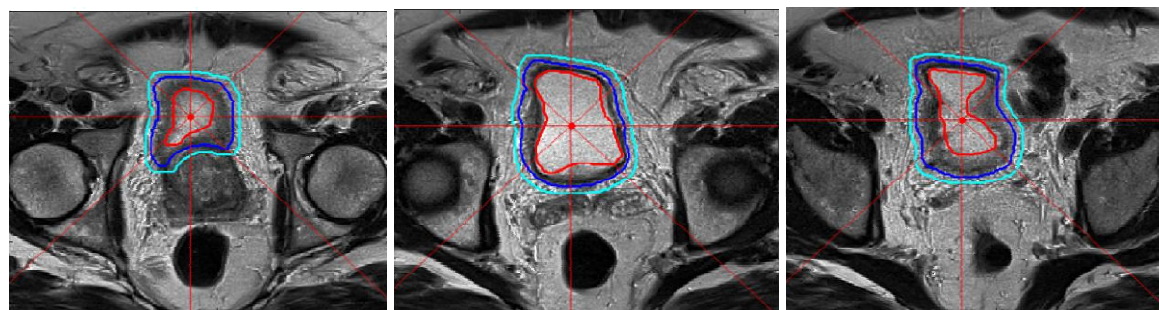


Figure 2. Three-layer shell-like structure and 8 radial sectors placed about the bladder on serial T2-weighted MR images in one representative patient. Three slices through the lower, middle and upper part of the bladder are displayed.

### 2.3 Feature extraction

According to the above definitions for the shells and sectors of the bladder, each patient had 8 sectors and each sector had three shells as shown in Figure 2. The image-based features including intensity and texture properties were then extracted from each sector and each shell for all patients. The texture information included the local binary pattern (LBP) and those derived from gray level co-occurrence matrix (GLCM) [4]. The GLCM features included six texture properties including energy, maximum probability, contrast, inverse difference moment, and correlation [5]. Four different versions of LBP features were computed including the original LBP [6], median LBP [7], uniform LBP [8], and neighbor intensity LBP [9]. In general, each sector yields 42 intensity properties, 672 LBP texture properties, and 15,120 GLCM texture properties. In total, 15,834 features were extracted from each sector.

### 2.4 Optimal biomarker selection

Each sector of the bladder from each patient had a reference standard T stage based on expert radiology qualitative MR image review and cystectomy histopathologic results, and each patient had an overall reference standard T stage similarly based on MRI and histopathology results.

After all the intensity and texture features were extracted at the patient level and sector level, an optimal feature set was selected from all extracted features using an optimal biomarker approach [10] to classify patients into the two T stage groups. This small optimal feature set was selected according to the following steps:

1. A small set of features with low (specified level of) correlation to all other features is selected as a subset.
2. A subset of features from the whole set that is capable of separating the two patient groups of interest is then extracted. Each feature is tested on its own for its ability to separate groups by using t-tests.
3. The intersection between the two subsets above in 1 and 2 is selected as the final selected feature set.

After the optimal feature set was determined, the accuracy of the classification into two T stage groups was evaluated at the patient level and at the sector level by using a leave-one-out strategy. A support vector machine (SVM) was selected as a classifier. Testing data sets in the leave-one-out strategy have no intersection with the training data sets used for optimal feature selection and SVM classification. Sensitivity, specificity, accuracy of prediction, and area under the receiver operating characteristic curve (AUC) are computed to describe the predictive performance of optimal feature sets consisting of different numbers of optimal features.

## 3. RESULTS

### 3.1 Image Data

This retrospective study was conducted following approval from the Institutional Review Board at the Hospital of the University of Pennsylvania along with a Health Insurance Portability and Accountability Act (HIPAA) waiver. Pelvic axial T2-weighted fast spin echo MR image data sets without gross motion artifacts from 65 adult bladder cancer patients (47 men, 18 women, mean age  $65.6 \pm 10.5$ ) acquired on 1.5-3.0 Tesla MRI scanners were utilized for this study. The image sizes varied from  $268 \times 208$  to  $512 \times 448$  with 23-65 slices, and the voxel sizes varied from  $0.62 \times 0.62 \times 4 \text{ mm}^3$  to  $1.48 \times 1.48 \times 12 \text{ mm}^3$ . The repetition time (TR) ranged from 1000-6680 msec, and the echo time (TE) ranged from 80-93 msec. 4 patients were imaged prior to transurethral resection of bladder tumor (TURBT), 27 patients were imaged after TURBT but prior to chemotherapy treatment, and 34 patients were imaged after TURBT and chemotherapy.

At the patient level, 31 patients comprised group 1 (T stage  $\leq$  T2, with primary tumor locally confined to the bladder) and 34 comprised group 2 (T stage  $>$  T2, with primary tumor locally extending beyond the bladder). In particular, 10 patients were stage T0, 3 patients were stage Ta, 5 patients were stage Tis, 5 patients were stage T1, 8 patients were stage T2, 24 patients were stage T3 (16 T3a and 8 T3b), and 10 patients were stage T4 (7 T4a, and 3 T4b).

At the sector level, 401 sectors comprised group 1 and 119 sectors comprised group 2. In particular, 289 sectors were stage T0, 3 sectors were stage Ta, 18 sectors were stage Tis, 29 sectors were stage T1, 62 sectors were stage T2, 88 sectors were stage T3 (52 T3a and 36 T3b), and 31 sectors were stage T4 (17 T4a and 14 T4b).

### 3.2 Experimental results

The size of the selected optimal feature set depends on the feature selection parameters [10]. The optimal biomarker feature sets from a minimum of 9 features to a maximum of 18 features are analyzed in this paper. For an optimal biomarker feature set with 9 features, and the AUC value at the sector and patient level were 0.813 and 0.806, respectively. The derived optimal biomarker feature set included only features from texture properties and originated from the middle shell. The optimal features were as follows:

- 1, 2. Kurtosis from uniform LBP with radius 3 and neighborhood 8 and 12.
- 3, 4. Median from contrast GLCM with the window size of 3x3 and 5x5.
- 5, 6. High quartile from correlation GLCM with the window size of 7x7 and radius 2 and 3.
7. High quartile from contrast GLCM with the window size of 3x3.
- 8, 9. High quartile from contrast GLCM with the window size of 5x5 and bins 5 and 10.

## 4. CONCLUSIONS

In this paper, an optimal biomarker approach is presented to select a small highly independent feature set in order to separate bladder cancer patients into two primary tumor (T) stage groups ( $\leq$  T2 vs.  $>$  T2). The method achieves an accuracy of up to 82%, including patients who have previously undergone TURBT or neoadjuvant chemotherapy. According to the results, all optimal biomarker features selected were extracted from the texture properties. In other words, the MRI standardized image intensity properties did not have a significant impact for distinguishing bladder cancer patients into these two groups. The selected texture properties included two types of features: from local binary pattern (LBP) and gray-level co-occurrence matrix (GLCM). The selected features were all extracted from the middle shell, which contains the bladder wall as well as foci of bladder cancer.

Future research may include extraction of more features from other MR imaging sequences such as T1-weighted, diffusion-weighted, and post-contrast T1-weighted images, as well as other less commonly used texture properties such as b-scale, t-scale, and g-scale, and histogram of gradients to improve the diagnostic accuracy of this approach.

## ACKNOWLEDGEMENTS

This work was partly funded by grants from Alan Wolson Fund at the Abramson Cancer Center, University of Pennsylvania, Philadelphia, United States.

## REFERENCES

- [1] R. Siegel, K. D. Miller, and A. Jemal, "Cancer statistics, 2017", *CA: a cancer journal for clinicians*, vol. 67, no. 1, pp. 7–30, 2017
- [2] L. G. Nyul, J. K. Udupa et al., "On standardizing the MR image intensity scale," *Magnetic Resonance in Medicine*, vol. 1081, 1999.
- [3] G. Grevera, J. Udupa, D. Odhner, Y. Zhuge, A. Souza, T. Iwanaga, and S. Mishra, "Cavass: a computer-assisted visualization and analysis software system," *Journal of digital imaging*, vol. 20, no. 1, p. 101, 2007.
- [4] R. M. Haralick, K. Shanmugam et al., "Textural features for image classification," *IEEE Transactions on systems, man, and cybernetics*, no. 6, pp. 610–621, 1973.
- [5] M. Sonka, V. Hlavac, and R. Boyle, *Image processing, analysis, and machine vision*. Cen-gage Learning, 2014.
- [6] T. Ojala, M. Pietikainen, and D. Harwood, "Performance evaluation of texture measures with classification based on Kullback discrimination of distributions," in *Pattern Recognition, 1994. Vol. 1-Conference A: Computer Vision & Image Processing, Proceedings of the 12th IAPR International Conference on IEEE*, vol. 1, pp. 582–585, 1994.
- [7] L. Liu, S. Lao, P. W. Fieguth, Y. Guo, X. Wang, and M. Pietikainen, "Median robust extended local binary pattern for texture classification," *IEEE Transactions on Image Processing*, vol. 25, no. 3, pp. 1368–1381, 2016.
- [8] T. Ojala, M. Pietikainen, and T. Maenpaa, "Multiresolution gray-scale and rotation invariant texture classification with local binary patterns," *IEEE Transactions on pattern analysis and machine intelligence*, vol. 24, no. 7, pp. 971–987, 2002.
- [9] L. Li, P. W. Fieguth, and G. Kuang, "Generalized local binary patterns for texture classification." *BMVC*, vol 123, pp. 1–11, 2011.
- [10] Y. Tong, J. K. Udupa, S. Sin, Z. Liu, E. P. Wileyto, D. A. Torigian, and R. Arens, "MR image analytics to characterize the upper airway structure in obese children with obstructive sleep apnea syndrome," *PloS one*, vol. 11, no. 8, 2016.
- [11] Vargas HA, Akin O, Schoder H, Olgac S, Dalbagni G, Hricak H, Bochner BH. "Prospective evaluation of MRI, (1)C-acetate PET/CT and contrast-enhanced CT for staging of bladder cancer". *Eur J Radiol*. 81(12), 4131-7, 2012.